Advanced Experimental Mechanics, Vol.3 (2018), 111-117

Two-dimensional Velocity Measurement Downstream of the Double Bend Pipe using Phased Array Ultrasonic Velocity Profiler

San SHWIN[1], Ari HAMDANI[2], Hideharu TAKAHASHI[2] and Hiroshige KIKURA[2]

[1] Graduate School of Science and Engineering, Tokyo Institute of Technology, Tokyo 152-8550, Japan
[2] Laboratory for Advanced Nuclear Energy, Tokyo Institute of Technology, Tokyo 152-8550, Japan

(*Received 10 January 2018; received in revised form 2 May 2018; accepted 2 May 2018*)

Abstract: In the present study, an experimental investigation is performed to obtain two-dimensional velocity field of the turbulent flow through the double bend pipe outlet. The main objective of the study is to investigate the velocity fluctuation in the recirculating flow region on the double bend pipe layout. Phased Array Ultrasonic Velocity Profiler is applied to obtain two-dimensional velocity field in a turbulent flow condition. In a water circulation piping system, the experiments are conducted in the turbulent flow condition, Reynolds number Re = 10,000. The measurement positions are located x/D = 1 and 1.5 (D = 50 mm) downstream of the double bent pipe outlet. Two-dimensional velocity field from the measurement result of Phased Array is compared with Particle Image Velocity (PIV) method. The reattachment point of the recirculating flow is found at the position x/D = 1. The axial and radial velocity fluctuations are analyzed near the reattachment point. The flow distortion and flow-accelerated phenomenon occur at the measurement positions downstream of the double bend pipe outlet.

Keywords: Two-dimensional velocity profile, Recirculating flow, Reattachment point, Flow distortion

1. Introduction

In fluid dynamic engineering, some researchers are studying the characteristic of swirling turbulent flow in the circular pipe or the rectangular channel due to its complexity. Turbulent flow can be found in engineering process such as in gas cyclone [1], turbine [2], and rod bundle in a nuclear reactor [3]. The recirculated swirling flow could also occur just downstream of the elbow or 90-degree bend pipe. The bent pipe can be encountered in many piping systems of the industries. Under the recirculating flow condition, the significant pressure fluctuation and the high-velocity fluctuation happen in the elbows, and these are sources of flow-induced vibration (FIV) [4]. FIV can cause the corrosion phenomenon of the pipe wall, and the pipe break accident may occur in a piping system of the industries and the power plants. Therefore, the characteristic of flow field and velocity fluctuation are significant issues for the pipeline safety.

In the previous studies, the influence of swirling flow was investigated downstream of elbow and orifice in different swirl intensities [5]. In that experiment, the effect of swirling flow on the pipe wall thinning was observed by using plaster dissolution method and the velocity field was visualized using stereo particle image velocimetry (PIV). Moreover, the influence of elbow curvature on flow structure of the elbow outlet under high Reynolds number condition was investigated to get the information of velocity fluctuation and flow-induced vibration [6]. The flow-induced vibration (FIV) occurs, especially in a short-elbow pipe. Therefore, Mizutani *et al.* [7] investigated the influence of inlet condition upstream the triple elbow. Particle Image Velocimetry (PIV) was used for the velocity flow mapping, and the tangential injection method was used to generate the fluid swirling flow in their study. The triple elbow with short curvature radius was used to be close to an actual condition and to accumulate knowledge towards optimization of a prospective piping layout in the conceptual design of Japan Sodium Fast Reactor (JSFR) [8]. In the previous studies, the researchers mostly used the optical system to measure the velocity field and velocity fluctuation. However, the optical system has some challenges to apply in non-transparent wall channel or pipe. Also, it is difficult for the applications in actual plant process. On the other hand, another measurement technique should be developed to evaluate the velocity field and velocity fluctuation. The developed measurement technique should be multidimensional and can be applied in the non-transparent conditions.

Takeda [9] developed Ultrasonic Velocity Profiler (UVP) to measure instantaneous velocity profile for non-transparent media and opaque liquid flows. Originally, conventional UVP method only measures one-dimensional velocity profile in the measurement line. In the case of two-dimensional velocity vector measurement, Takeda and Kikura [10] investigated velocity field of the mercury flow using UVP system with multiple transducers. Nevertheless, the measurement system using multiple transducers is quite large as the number of transducers is increased. To minimize this problem, the authors had developed Phased Array Ultrasonic Velocity Profiler (Phased Array UVP). In Phased Array UVP, the sensor has multiple ultrasonic piezoelectric elements and ultrasound beam can be steered to a specific angle by controlling time delay of ultrasound transmission from each piezoelectric element. Therefore, velocity profiles can be measured in multiple measurement lines. For the flow mapping, Fukumoto *et al.* [11] confirmed Phased Array UVP for velocity flow mapping for detecting water leakage in the tank.

The main objective is to investigate velocity fluctuation of recirculating flow downstream of the double bend pipe applying Phased Array UVP. Two-dimensional velocity field from the measurement of Phased Array UVP is compared with PIV method and the axial and radial velocity fluctuation are analyzed in one-dimensionally.

2. Measurement System and Experimental Apparatus

2.1 Two-dimensional velocity by phased array UVP

Phased Array UVP based on Doppler shift frequency detection along ultrasound beamlines. Phased array sensor emits an ultrasonic pulse, and each piezoelectric element of sensor receives the echo reflected from the surface of a particle. When adjacent elements emit within a close second, interference of wavefronts occurs as shown in Fig.1 (a). The exciting element emits a spherical ultrasonic wave. Figure 1 (b) shows a schematic diagram of phased array sensor which l is element length, d is inter-element spacing, and w is element width. The pattern of the interference depends on the time delay, the steering angle of ultrasonic beam can be changed at the time delay Δt. The steering angle θ_s and the time delay Δt is related with the speed of sound in a medium c and inter-element spacing d as shown in Eq. (1).

$$\theta_s = \sin^{-1}\left[\frac{c\Delta t}{d}\right] \tag{1}$$

Basic equation of Doppler shift is derived from Doppler equation as shown below:

$$f_d = \frac{2sf_0}{c} \tag{2}$$

where f_d is the Doppler frequency, s is the speed at which object is approaching the transducer, f_0 is the basic frequency of the transducer, and c is the speed of sound in the medium, i.e., water. If the object is moving at an angle θ to the transducer, then $s = V \cos\theta$. By substitution, we get the Doppler shift equation for a single transducer:

$$f_d = \frac{2f_0 V\cos\theta}{c} \tag{3}$$

Equation (3) can be rewritten as:

$$f_d = \left(\frac{f_0 V}{c}\right)2\cos\theta \tag{4}$$

where 2cos θ applies to a roundtrip Doppler shift using a single transducer. If two transducers are used, one receiver and one transmitter, as shown in Fig. 2(a). Then, 2cos θ becomes cos θ + cos γ, where θ is the angle between the transmitter and the vector V, and γ is the angle between the receiver and the vector V. Moreover, $\alpha = \theta$-γ, where α is the angle between the transmitter and receiver, then cos γ = cos (θ- α).

The Doppler equation becomes:

$$f_d = \left(\frac{f_0 V}{c}\right)\left[\cos\theta + \cos(\theta-\alpha)\right] \tag{5}$$

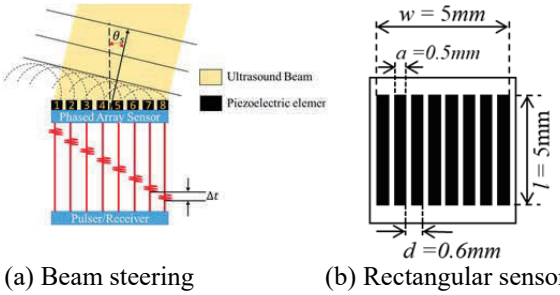

(a) Beam steering (b) Rectangular sensor

Fig. 1 Beam steering principle and sensor geometry

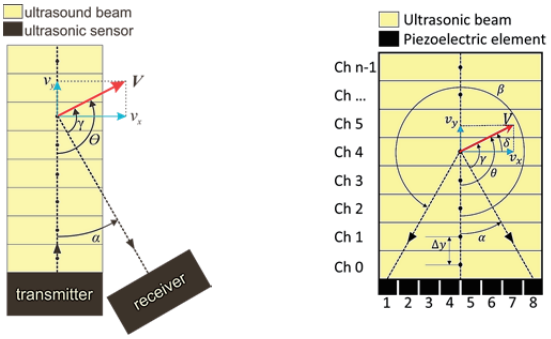

(a) Two transducer system (b)Vector reconstruction

Fig. 2 Multi-element system and vector reconstruction

Using the trigonometric identity:

$$\cos(\theta-\alpha) = \cos\theta\cos\alpha + \sin\theta\sin\alpha \tag{6}$$

The Doppler Eq. (5) becomes:

$$f_d = \left(\frac{f_0 V}{c}\right)\left[\cos\theta + \cos\theta\cos\alpha + \sin\theta\sin\alpha\right] \tag{7}$$

In this paper, phased array sensor is used as transmitter and receiver (transceiver). As shown in Fig. 2(b), the number of piezoelectric elements is eight. These eight elements transceiver transmit ultrasound beam at the same time or delayed for certain time to get steering angle, then the beams from these transceivers will interference pattern forming (beamforming) into one beam.

For measuring two-dimensional velocity vector, the development system uses two piezoelectric elements as transceivers to calculate the actual velocity magnitude and angle from the returned signal at specific measuring volume, i.e., Channel 4 (Ch 4) as shown in Fig.2 (b). The Doppler shift equation for the piezoelectric element number 8 is identical to Eq (7):

$$f_{d8} = \left(\frac{f_0 V}{c}\right)\left[\cos\theta + \cos\theta\cos\alpha + \sin\theta\sin\alpha\right] \tag{8}$$

where f_{d8} is the Doppler frequency received by the piezoelectric element number 8 at angle α (measured clockwise from the axis of the transmitting beam), f_0 is basic frequency, V is the magnitude of the velocity of the particle travelling at angle θ (measured clockwise from the axis of the transmitting beam), and c is the speed of sound in fluid.

The Doppler shift equation for the piezoelectric element number 1 is:

$$f_{d1} = \left(\frac{f_0 V}{c}\right)\left[\cos\theta + \cos\theta\cos\alpha + \sin\theta\sin\alpha\right] \tag{9}$$

where f_{d1} is the Doppler frequency received by the piezoelectric element number 1 at angle β (measured clockwise from the axis of the transmitting beam), and all other terms are identical to those of the piezoelectric element number 8.

The signals from both of these transceivers are demodulated with the transmitted frequency f_0 to produce four quadrature signals. It should be noted that at a given depth (channel) from the surface of both piezoelectric elements f_0, c, α, and β are all-constant due to the fixed geometry of the piezoelectric elements. The real velocity

vector V is calculated by multiplying the four-quadrature signals from the two transceivers elements number 1 and 8. The multiplying produces two subcomponents, which are the sum of the frequencies and the difference between the frequencies. Using trigonometry:

$$\cos f_{d1}\cos f_{d8}=\frac{1}{2}\left[\cos\left(f_{d1}+f_{d8}\right)+\cos\left(f_{d1}-f_{d8}\right)\right] \quad (10)$$

From Eq. (8) and Eq. (9), we will get the equations for the sum and difference as follow:

$$f_{d1}+f_{d8}=\frac{f_0V}{c}\begin{bmatrix}\cos\theta+\cos\theta\cos\beta+\sin\theta\sin\beta+\\ \cos\theta+\cos\theta\cos\alpha+\sin\theta\sin\alpha\end{bmatrix} \quad (11)$$

If $\sin\beta$ = -$\sin\alpha$ and $\cos\beta=\cos\alpha$, then Eq. (11) becomes

$$f_{d1}+f_{d8}=\frac{f_0V}{c}\begin{bmatrix}\cos\theta+\cos\theta\cos\beta+\sin\theta\sin\beta+\\ \cos\theta+\cos\theta\cos\alpha+\sin\theta\sin\alpha\end{bmatrix}$$

$$f_{d1}+f_{d8}=\frac{f_0V}{c}\left[2\cos\theta\left(1+\cos\theta\right)\right] \quad (12)$$

$$f_{d1}+f_{d8}=\frac{2f_0}{c}\left(1+\cos\theta\right)V\cos\theta$$

$$f_{d1}-f_{d8}=\frac{f_0V}{c}\begin{bmatrix}\cos\theta+\cos\theta\cos\beta+\sin\theta\sin\beta-\\ \cos\theta-\cos\theta\cos\alpha-\sin\theta\sin\alpha\end{bmatrix} \quad (13)$$

If $\sin\beta$ = -$\sin\alpha$ and $\cos\beta=\cos\alpha$, then Eq. (13) becomes

$$f_{d1}-f_{d8}=\frac{f_0V}{c}\begin{bmatrix}\cos\theta+\cos\theta\cos\beta+\sin\theta\sin\beta-\\ \cos\theta-\cos\theta\cos\alpha-\sin\theta\sin\alpha\end{bmatrix}$$

$$f_{d1}-f_{d8}=\frac{f_0V}{c}\left[-2\sin\theta\sin\alpha\right] \quad (14)$$

$$f_{d1}-f_{d8}=-\frac{2f_0}{c}\sin\alpha V\sin\theta$$

If $V_x=V\sin\theta$ and $V_y=V\cos\theta$, then from Eq. (12) and (14):

$$V_x=-\frac{\left(f_{d1}-f_{d8}\right)}{2f_0}\frac{c}{\sin\alpha} \quad (15)$$

$$V_y=\frac{\left(f_{d1}+f_{d8}\right)}{2f_0}\frac{c}{\left(1+\cos\alpha\right)} \quad (16)$$

Since these V_x and V_y are orthogonal, the real magnitude can be determined by vector addition, and simple trigonometry can determine the angle:

$$V=\sqrt{V_x^2+V_y^2} \quad (17)$$

$$\delta=\tan^{-1}\left(\frac{V_y}{V_x}\right) \quad (18)$$

The spatial resolution or channel distance is defined as:

$$\Delta y=\frac{n_{cycle}}{2f_0}c \quad (19)$$

where Δy is channel distance, n_{cycle} is number of cycles per pulse, c is the speed of sound, and f_0 is the basic frequency of the transducer.

Hardware system of Phased Array UVP is showed in Fig. 3. National Instrument LabVIEW program is used to control Phased Array UVP and reconstruct two-dimensional velocity vector.

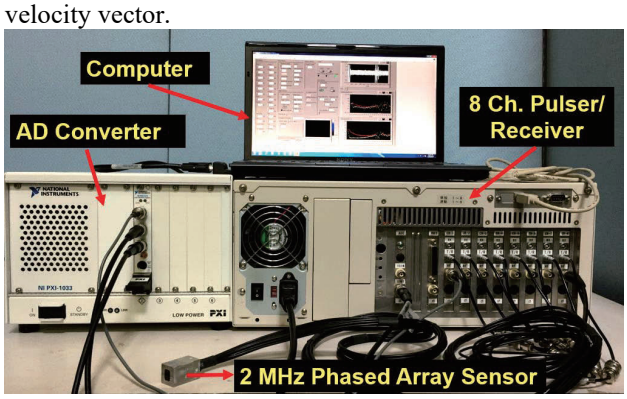

Fig. 3 Hardware system of Phased Array UVP

The hard ware system consists of a 2 MHz phased array sensor with eight piezoelectric elements, 8-channel pulse receiver, analog to digital converter and personal computer to control the pulse receiver and analyze echo signal from the digitizer.

2.1.1 *Near-field effect of phased array sensor*

In Phased Array UVP, we have to consider the effect of the near field length (L). The high oscillation burst occurs near the active elements surface. It can influence the accuracy of the measurement close to the sensor in the near-field region. The near-field of phased array sensor has been investigated numerically as shown in Fig.4. Near field length depends on the width of piezoelectric element w and the wavelength of the ultrasound pulse λ [12]. From Eq. (20), we can estimate the near field length of the phased array sensor.

$$L=\frac{kw^2}{8\lambda} \quad (20)$$

where, k is factor and w is piezoelectric element width (w = 5mm). For the rectangular sensor, the aspect ratio of element width and length (w/l) is 1. Corresponding to this ratio, factor k is around 1.37 as shown in Fig.5. In case of 2 MHz sensor, the wavelength λ is 0.74 mm and the near field length is 5.78 mm from the element surface.

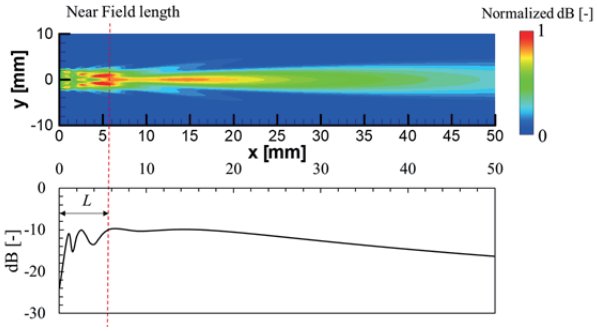

Fig. 4 Near-field leangth (L) of sound pressure

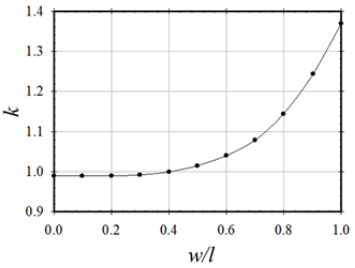

Fig. 5 Correction factor (k) of rectangular sensor

2.2 Experimental apparatus and procedures

The experiment was conducted in a water circulation system, which consisting of the cooling system to keep constant temperature. The water temperature is keep in 25 ˚C for sound speed c = 1480 m/s. The inner diameter of the pipe is 50 mm and made of acrylic. The distance from the inlet to double bend is 40D (D = 50 mm). In that position, the fluid is in the fully developed turbulent pipe flow condition. The double bent pipe is utilized to investigate the recirculating flow. The double bent pipe has a bent angle of 90 degrees and curvature radius R_c = 25 mm. The schematic view of the measurement position is shown in Fig. 6(a).

For this experiment, we measured in the axial plane at x/D = 1 and x/D = 1.5 from the downstream of the second elbow to observe the flow acceleration phenomenon of recirculating flow in the reattachment point region. The water flows in the turbulent flow condition at Reynolds number (Re =10,000). The time transient temperature data is recorded using thermocouple during the measurements. Table 1 and 2 show the experimental and measurement system conditions

A phased array sensor, which has basic frequency 2 MHz, is installed through the pipe wall. Thus, there is a direct contact between sensor and fluid to overcome the refraction in pipe wall and fluid medium. The number of cycle in an ultrasound pulse is n_{cyle} = 2 and the spatial resolution is 0.74 mm.

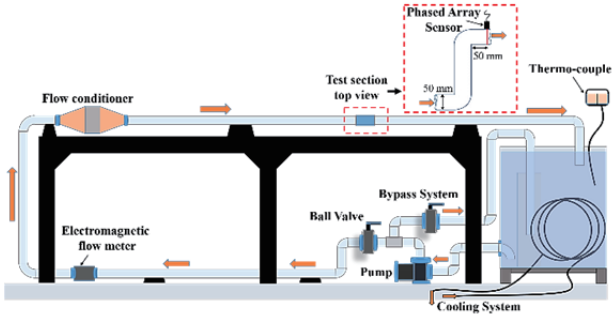

(a) Experimental facilities of a piping system

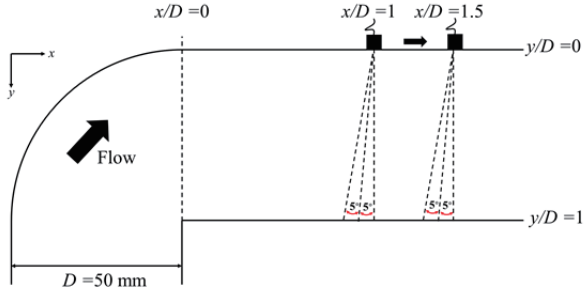

(b) Detail view of Phased Array UVP test section

Fig. 6 Schematic view of the experimental setup

Table 1 Experimental conditions

Parameters	Value
Reynolds numbers [-]	10000
Fluid (water) temperature [˚C]	25 ± 1
The radius of elbow curvature [mm]	25
Pipe diameter [mm]	50
Proximity between two elbows [mm]	300

The maximum steering angle of the phased array sensor is -10 degree to 0 degree. In the measurement positions, we measured three measurement lines, and the interval between each measurement lines is 5 degree as shown in Fig. 6 (b).

In addition, Particle Image Velocimetry (PIV) method is applied in this experiment to compare the results of Phased Array UVP. PIV system consisted of a laser (DANTEC DYNAMICS), High-Speed Camera (FastCam SA5). The camera is located at the top of the measurement region, and the laser beam emits from the side of the pipe through the pipe center to measure the axial plane of the fluid. PIV measurement section and the detail view of measurement section are shown in Figs. 7 and 8. In PIV method, High-Speed Camera captures the images of nylon tracer particles lightened by the laser sheet in working fluid. The total number of frames per one record was 5250, and the camera captured 750 frames per second. The image sizes are 110 mm ×110 mm (1024 pixel × 1024 pixel). The data from the images analysis in PIV Lab application by using MATLAB program. The reference region is 200 pixel × 24 pixels. Two-dimensional velocities are obtained by averaging 5250 subsequent images of the particles motion.

Table 2 Measurement parameters of Phased Array UVP

Parameters	Value
Frequency of Phased array sensor [MHz]	2
Number of cycle in a pulse [-]	2
Spatial resolution [mm]	0.74
Steering angle [degree]	-10˚, -5˚, 0˚
Pulse repetition frequency [kHz]	1
Number of repetition [-]	128
Time resolution [s]	0.128
Number of velocity profiles	10,000

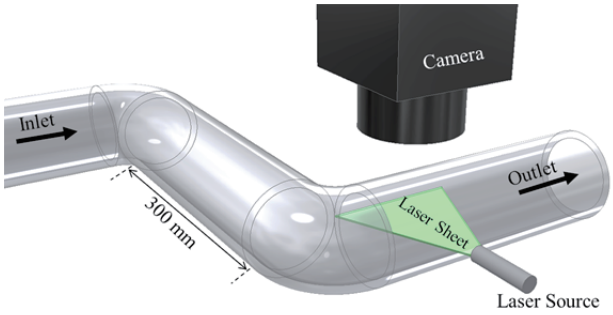

Fig. 7 PIV measurement section

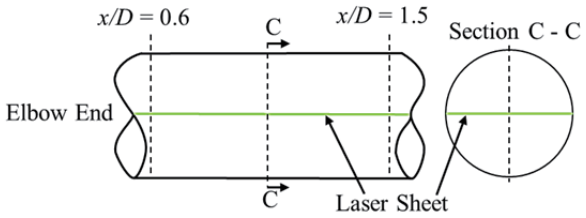

Fig. 8 Detail view of PIV test section

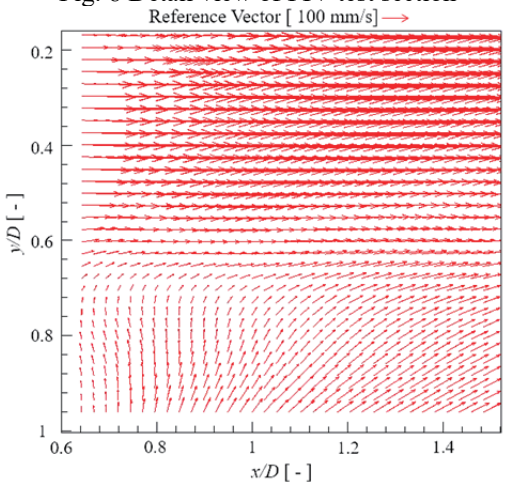

Fig. 9 Average velocity vector (PIV)

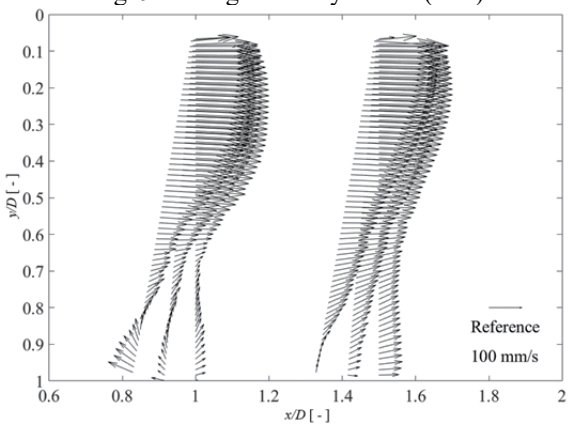

Fig. 10 Average velocity vector (Phased Array UVP)

3. Results and Discussion

Figure 9 shows two-dimensional velocity vector from PIV measurement. The measurement area starts from *x/D = 0.6* to *x/D = 1.55*. The flow distortion and recirculation flow occur downstream region of double bend pipe outlet. Therefore, two different flow patterns (*y/D* = 0.2 to *y/D* = 0.6) and (*y/D* = 0.7 to *y/D* = 0.9) can be recognized in the flow field. We can assume that the recirculating flow region is located from the sharp bend curvature to *x/D* = 1 according to the direction of the velocity vector. The forward flow starts around *x/D* = *1* and continues to the downstream region.

Figure 10 shows two-dimensional velocity vector from Phased Array UVP measurement at *x/D* = 1 and *x/D* = 1.5 downstream of the double bend pipe. In each measurement position, we measured three measurement lines, and the interval between each measurement lines is 5 degree. The vector field cannot be measured near the oscillation boundary of the phased array sensor. In the experiment, the near-field oscillation boundary is observed from *y/D* = 0 to *y/D* = 0.08. The ten thousand instantaneous velocity vectors are averaged in each measurement line because, in the turbulent flow condition, the velocity fluctuation is very high downstream of the double bend pipe. In the position of *x/D* = 1, velocity vectors in the first two measurements are reversed flow direction at the bottom part of measurement lines, and the main flow region is located from *y/D* = 0 to *y/D* = 0.8. We can observe the reattachment point at zero degree perpendicular measurement line of *x/D* = 1. It means that the forward flow starts from that measurement line and at *x/D* = 1.5 the reverse flow is disappeared but the flow pattern is still asymmetric.

Two measurement results are compared in Fig. 11. The black velocity vector is from Phased Array UVP, and the red velocity vector is from PIV. To compare the measurements result, the velocity vector in PIV results are selected at the same spatial resolution and same measurement line as Phased Array UVP velocity vector. In PIV measurement result, the velocity vector cannot be analyzed close to the pipe boundary from *y/D* = 0 to *y/D* = 0.16 because of pipe curvature effect and the reflection of laser sheet. In the main flow area, flow pattern are same in both case, but the velocity magnitude in PIV is a bit larger than Phased Array UVP. However, it is not much different if we compare in one-dimensional case. In the recirculating flow region, the reverse flow pattern can be seen in Phased Array UVP result.

In PIV results, the reverse flow vector field is not totally reverse. However, we can assume that the recirculation flow region is located from the elbow end to *x/D* = 1.

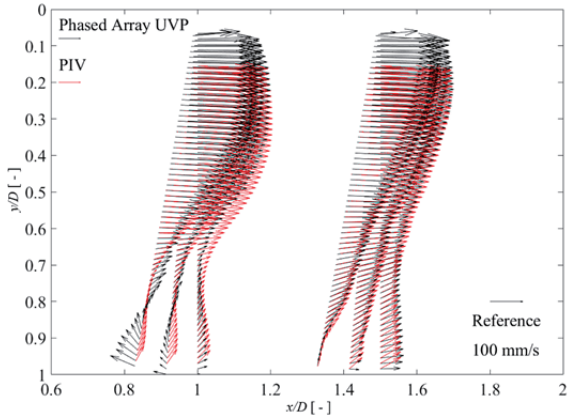

Fig. 11 Phased Array UVP and PIV measurement results in two-dimenisonal vector

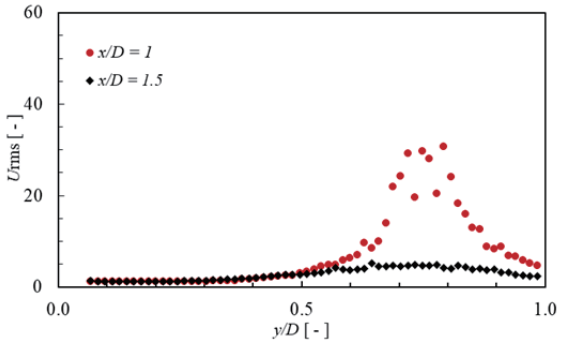

(a) Root mean square of axial velocity

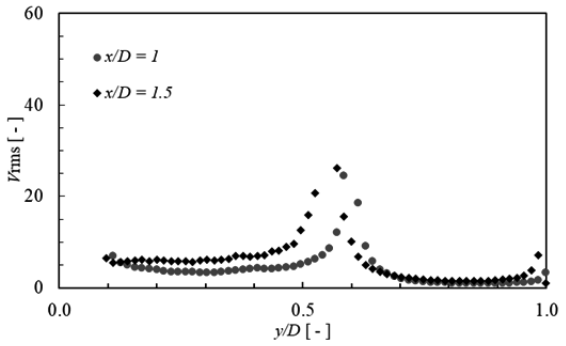

(b) Root mean square of radial velocity

Fig. 12 Velocity fluctuation analysis (Phased Array UVP)

Velocity fluctuation is analyzed from instantaneous velocity vector from Phased Array UVP measurement at the perpendicular 0 degree measurement line in x/D = 1 and x/D = 1.5 positions. Figure 11 shows the root mean square (RMS) value of axial velocity (U_{rms}) and radial velocity (V_{rms}). RMS value of axial and radial velocity is important to analyze the velocity fluctuation in the turbulent flow. From U_{rms} analyzed graph, the axial velocity fluctuation at the position x/D =1 is very high between y/D = 0.6 and y/D = 0.8 (see in Fig.12 (a)). However, the axial velocity fluctuation at the position x/D = 1.5 is almost stable compare with x/D = *1*. It means that the high velocity fluctuation occurs at the boundary of the main flow and recirculating flow. In Fig. 12 (b), the radial velocity fluctuation is high at the center of the pipe. When the fluid enters the elbow and touches the curved wall, the flow direction changes and the circular flow well-known as the secondary flow in the bent pipe occurs. Therefore, at the core of the flow (near the pipe center), the high radial velocity fluctuation is induced in x/D = 1 and x/D = 1.5.

4. Conclusions

In order to understand the velocity distribution of turbulent flow just downstream of the double bent pipe outlet, the measurement of the two-dimensional velocity vector is carried out by Phased Array UVP system and PIV. The flow distortion and recirculating flow occur in the measurement region downstream of the double bend pipe. From both measurement results, the recirculating flow region was observed and the reattachment point occurs around x/D = 1. In the velocity fluctuation analysis, the axial velocity fluctuation apparently occurs at the boundary of the main flow and the recirculating flow. The radial velocity fluctuation occurs at the center of the pipe.

Nomenclature

a	single element width [mm]
b	total element width [mm]
c	sound speed in water[m/s]
d	inter element spacing [mm]
l	piezoelectric element length [mm]
k	correction factor [-]
w	piezoelectric element width [mm]
s	speed of particle [-]
D	pipe diameter [mm]
L	Near-field length [mm]
f_{di}	Doppler shift frequency, which is observed at i^{th} channel elements [Hz]
f_0	basic frequency of phased array sensor [Hz]
Re	Reynolds number ($Re = UD/\nu$) [-]
R_c	curvature radius of the elbow [mm]
V	bulk velocity [mm/s]
L	Near-field oscillation [mm]
n_{cycle}	Number of cycle in a pulse [-]
U_{rms}	axial velocity rms value [-]
V_{rms}	radial velocity rms value [-]
$\vec{V}$	velocity vector of the moving particle [mm/s]
θ_s	phased steering angles [degree]
$\propto \beta\ \delta$	angles between the transmitter and receiver [degree]
Δt	time delay of ultrasound pulse
Subscripts	
x, y	Coordinates [mm]

Acknowledgment

I would like to appreciate JICA (Japan International Cooperative Agency), for the scholarship.

References

[1] Hoekstra, A. J., Derksen, J. J. and Van Den Akker, H. E. A.: An experimental and numerical study of turbulent swirling flow in gas cyclones, *Chemical Engineering Science*, **54**-13-14 (1999), 2055-2065.

[2] Susan-Resiga, R., Ciocan, G. D., Anton, I. and Avellan, F.: Analysis of the swirling flow downstream a Francis turbine runner, *Journal of Fluids Engineering*, **128**-1 (2006), 177-189.

[3] McClusky, H. L., Holloway, M. V., Beasley, D. E. and Conner, M. E.: Development of swirling flow in a rod bundle subchannel, *Journal of Fluids Engineering*, **124**-3 (2002), 747-755.

[4] Chen, S. S.: Flow-induced in-plane instabilities of curved pipe, *Nuclear Engineering and Design*, **23**-1 (1972), 29-38.

[5] Takano, T., Ikarashi, Y., Uchiyama, K., Yamagata, T. and Fujisawa, N.: Influence of swirling flow on mass and momentum transfer downstream of a pipe with elbow and orifice, *International Journal of Heat and Mass Transfer*, **92** (2016), 394-402.

[6] Ono, A., Kimura, N., Kamide, H. and Tobita, A.: Influence of elbow curvature on flow structure at elbow outlet under high Reynolds number condition, *Nuclear Engineering and Design*, **241**-11 (2011), 4409-4419.

[7] Mizutani, J., Ebara, S. and Hashizume, H.: Evaluation of influence of the inlet swirling flow on the flow field in a triple elbow system, *International Journal of Hydrogen Energy*, **41**-17 (2016), 7233-7238.

[8] Ebara, S., Takamura, H., Hashizume, H. and Yamano, H.: Characteristics of flow field and pressure fluctuation in complex turbulent flow in the third elbow of a triple elbow piping with small curvature radius in three-dimensional layout, *International Journal of Hydrogen Energy*, **41**-17 (2016), 7139-7145.

[9] Takeda, Y.: Velocity profile measurement by ultrasound

Doppler shift method, *International Journal of Heat and Fluid Flow*, **7**-4 (1986), 313-318.
[10] Takeda, Y. and Kikura, H.: Flow mapping of the mercury flow, *Experiments in Fluids*, **32**-2 (2002), 161-169.
[11] Fukumoto, T., Tsukada, K., Ihara, T., Tsuzuki, N. and Kikura, H.: A study of phased array ultrasonic velocity profile monitor for flow rate measurement, *Proc. 21st International Conference on Nuclear Engineering*, Paper No. ICONE21-16601 (2013), 1-6.
[12] British Standards EN12668-2 Non-Destructive Testing: Characterization and verification of ultrasonic examination equipment, Part 2-Probes (2008), 47-48.